Experimental study of corrosion-induced degradation of reinforced concrete elements

Olfa Loukil, Lucas Adelaide, Véronique Bouteiller, Marc Quiertant, Thierry Chaussadent, Frédéric Ragueneau, Xavier Bourbon, Laurent Trenty

International RILEM Conference on Materials, Systems and Structures in Civil Engineering
Conference segment on Service life of cement-Based Materials and Structures
22-24 August 2016, Technical University of Denmark, Lyngby, Denmark

EXPERIMENTAL STUDY OF CORROSION-INDUCED DEGRADATION OF REINFORCED CONCRETE ELEMENTS

O. LOUKIL[(1)], L. ADELAIDE[(1)], V. BOUTEILLER[(1)], M. QUIERTANT[(2)], T. CHAUSSADENT[(3)], F.RAGUENEAU[(4)], X. BOURBON[(5)], L. TRENTY[(5)]

[(1)]*Université Paris-Est, MAST, SDOA, IFSTTAR, F-77447 Marne-la-Vallée, France.*
[(2)]*Université Paris-Est, MAST, EMMS, IFSTTAR, F-77447 Marne-la-Vallée, France.*
[(3)]*Université Paris-Est, MAST, CPDM, IFSTTAR, F-77447 Marne-la-Vallée, France.*
[(4)]*LMT/ENS Cachan/CNRS/Univ. Paris 6/PRES UniverSud, 94230 Cachan, France*
[(5)]*ANDRA, F-92298 Chatenay-Malabry, France*

Abstract

Corrosion of steel reinforcement is the main cause of damage for reinforced concrete structures. Iron oxides produced during the corrosion process can induce concrete cracking, loss of adhesion at the steel-concrete interface, loss of reinforcing bar cross-section and even spalling of the concrete cover.
In the presented research, the durability problems related to the corrosion of the reinforcement are investigated by combining experimental and numerical studies. However, this paper particularly focuses on the experimental methodology used for the time evolution of damages (steel corrosion products formation and crack patterns) induced by the accelerated corrosion test. The accelerated corrosion tests were carried out by applying a constant current between reinforcement used as an anode and a counter electrode. To control the corrosion process, electrochemical parameters (such as free corrosion potential, polarization resistance, electrical concrete resistance) were measured. The purpose of this paper is to determine the width and length of the cracks and their orientation according to the current density and time.
Keywords: Corrosion, cracks, iron, electrochemistry, finite element analysis

1 Introduction

Corrosion of steel reinforcement is one of the main causes of deterioration of existing reinforced concrete (RC) structures. The consequences of this phenomenon are degradation of

the steel/concrete bond, reduction of the steel rebar cross-section and concrete cover cracking [1]. This last phenomenon results from the production of oxides which occupy a volume two to seven times higher than the parent steel. Actually, when this production is greater than diffusion of iron oxide in the concrete, pressure increases at the interface between the surrounding concrete and the rebar [2] [3] and exerts tensile stresses in the concrete all along the corroding reinforcements. If these stresses exceed concrete tensile strength, the cracking initiates and propagates towards the outer surface leading to the delamination of the concrete cover [4] [5]. Due to the mechanical deleterious effect of the corrosion phenomenon, it is important to develop non-destructive techniques as well as predictive numerical modelling to assess the corrosion evolution of RC structures. This could help the structure's end users to provide an efficient maintenance policy. The main issue of this paper is to design a specific protocol to generate a "controlled" corrosion evolution versus time in order to bring some experimental evidences on the concrete cover cracking process due to corrosion and to determine relevant input parameters for the numerical modelling.

2 Experimental program

2.1 Materials and specimens

Twelve single-rebar specimens (500x125x100mm^3) were casted with a 600mm long and 20mm diameter steel deformed rebar. The reinforcement was positioned to obtain a 30mm concrete cover at two sides of the beam [Figure 1]. The specimens designed with a not symmetric location of the rebar aim to get closer to reality, to represent the heterogeneity of the mechanical environment of the reinforcement in a structure. A Portland cement and siliceous aggregates were used for the concrete composition with a water to cement ratio of 0.73. This ratio is representative of old reinforced concrete structures. Moreover, it allows the penetration of the chloride ions during the accelerated corrosion test.

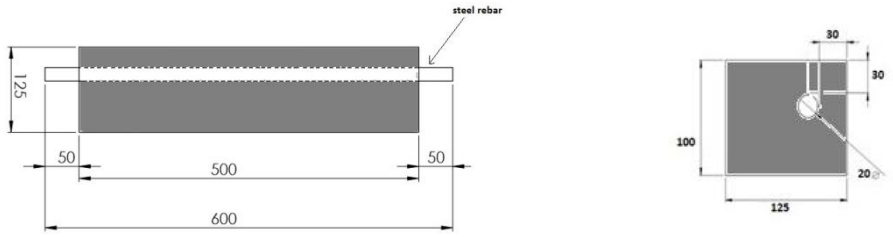

Figure 1. Schematic representation of RC specimens (dimensions in millimeters)

The cement type used for the concrete composition was CEM I 52.5 CP2 NF according to European standards. Concrete was prepared with aggregates having different particle size classes ((0/0.315 mm; 0.315/1 mm; 0.5/1 mm; 1/4 mm; 2/4 mm; 4/8 mm; 8/12 mm; 12.5/20 mm)). Compressive and tensile strengths were measured on concrete cylinders (160mm in diameter, 320mm in height) after 28 days according to NF EN 12390-3 [6] and NF EN 12390-

6 [7] standards. The mean compressive strength is 32 MPa ± 2.46, the tensile strength is 2.6 MPa ± 0.08 and the Young's modulus is 35 GPa ± 1.58. The Poisson's ratio is equal to 0.15.

2.2 Accelerated corrosion tests and monitoring system

The set-up used for accelerated corrosion test and the monitoring system are illustrated in [Figure 2]. RC samples were corroded using a power supply (Agilent 6614C, 100V, 0.5A) which delivered an imposed anodic current to the steel rebar. The counter electrode (cathode) consisted in an inert platinum titanium mesh (275mm long, 75mm wide) placed into a PVC tank containing the alkaline electrolyte (1 g/L of NaOH, 4.65 g/L of KOH, 30 g/L of NaCl) which was glued on the top side of the concrete (in the middle of the specimen). All the specimens were connected in series and a current density of 100 µA/cm² of steel (0.0172A for a steel surface area of 172.8 cm²: diameter 20mm and length 275mm) was applied during the chosen exposure time (7d, 14d, 21d, 28d and 35d). At the end of each considered exposure time, two specimens were disconnected from the electrochemical test set-up. One of the specimens was used for the non-destructive electrochemical characterization and the other one was dedicated to destructive measurements. The accelerated corrosion test was monitored using a data acquisition unit (Keysight 34970A): temperature, delivered constant current, each sample voltage and total voltage were recorded every two hours. Moreover, two cameras were used for the digital image acquisition of the front side of the two specimens subjected to a 35 days accelerated corrosion test.

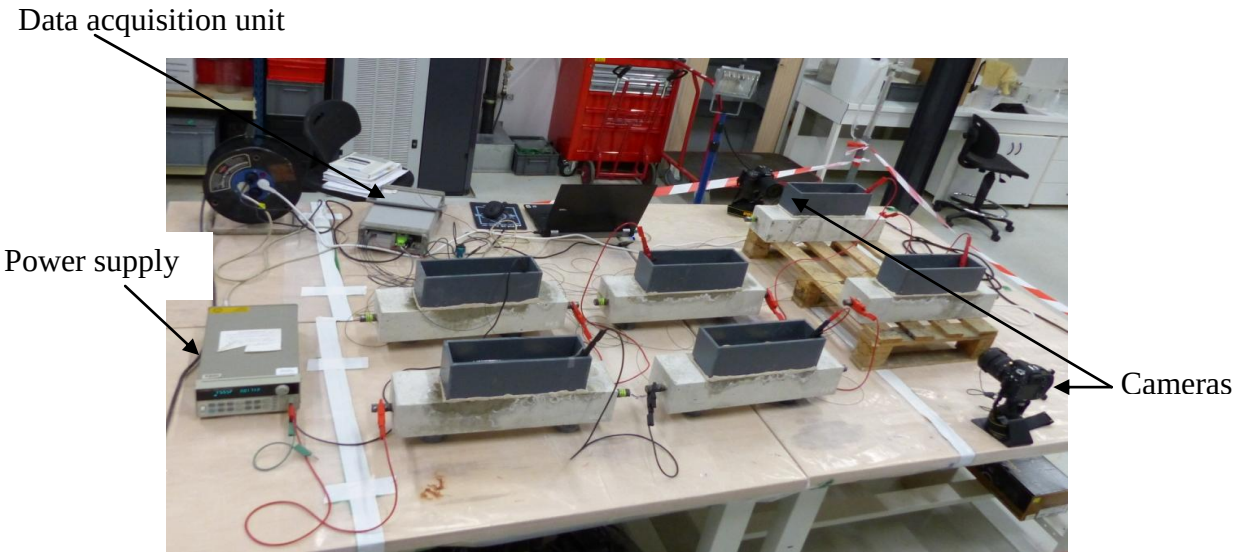

Figure 2. Accelerated corrosion and monitoring system

2.3 Electrochemical characterizations

In order to determine the corrosion state of the rebar before the accelerated test, half-cell potential measurements (E_{corr}) linear polarization resistance measurements (LPR) and impedance spectroscopy (Re) were carried out, using a potentiostat (Bio-Logic, PARSTAT

2263) and the usual electrochemical cell with three electrodes. The working electrode was the steel rebar, the reference electrode was a KCl saturated calomel electrode (SCE, 242 mV / SHE) and the counter electrode was a titanium platinum mesh [Figure 3]. The same electrolyte as for the accelerated corrosion test was used. Then the corrosion current density J_{corr} (µA/cm²) was calculated based on the following equation:

$$J_{corr} = \frac{B}{R_p \ S} \quad (1)$$

with *B* a constant (26mV), *Rp* (ohm) the linear polarization resistance and *S* (cm²) the steel surface (172.78 cm² in this study).

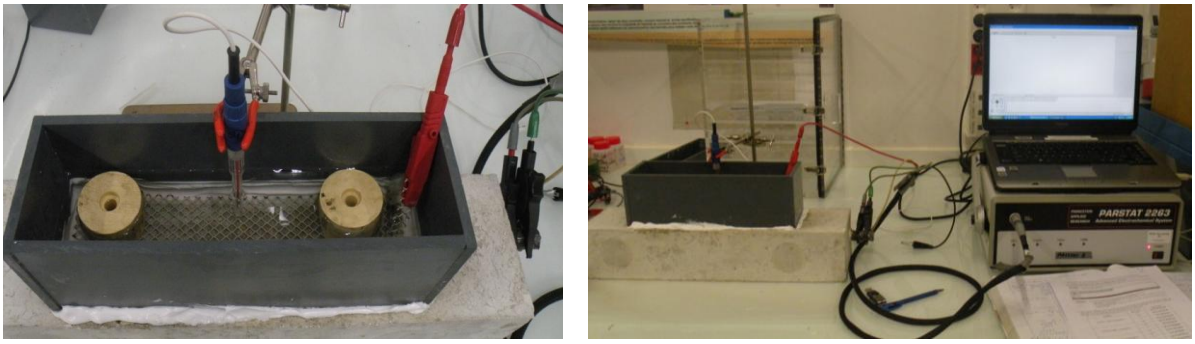

Figure 3. Electrochemical setup

2.4 Observation of corrosion products, of steel/concrete interface and estimation of the crack patterns

Visual observations

After the accelerated corrosion test, the specimens were observed and a special focus was made on the top and the front sides because of their lower concrete cover (30mm). Cracks opening were measured with a crack measuring magnifier (resolution 0.1mm) on these two surfaces. Then the specimens were sliced (125x100x20mm^3), considering corroded areas as illustrated in [Figure 4]. After 24h drying in an oven at 45°C, the slices were photographied and examined in order to characterize the crack pattern (angle and length) [Figure 5]. To determine the angular position, the methodology developed by Sanz-Merino [8] was adopted [Figure 5-a]. To estimate the length of the cracks in each cross-sections, the photographs of the cross-section and a circle graduated every centimeter were superimposed as shown in [Figure 5-b]. Moreover, the corrosion products embedding the rebar and filling the concrete cracks were analyzed. Then from both results an attempt was made to correlate what was seen on the concrete surface in 2Dimensions (by the bridge's owner) and what happened inside the concrete with an aim of 3Dimensions.

Scanning Electron Microscopy observations

The slices were then impregnated with an epoxy resin under vaccum (to prevent decohesion between concrete and steel when the corrosion damage was severe) and then cut into samples

which dimensions (2x4.5x4.5cm^3) fitted in the Scanning Electron Microscopy (SEM) observation room. A first goal is to determine the corrosion product thickness and their length circling the perimeter of the rebar. A second objective is to observe the crack pattern and the transfer of the oxides through the cracks.

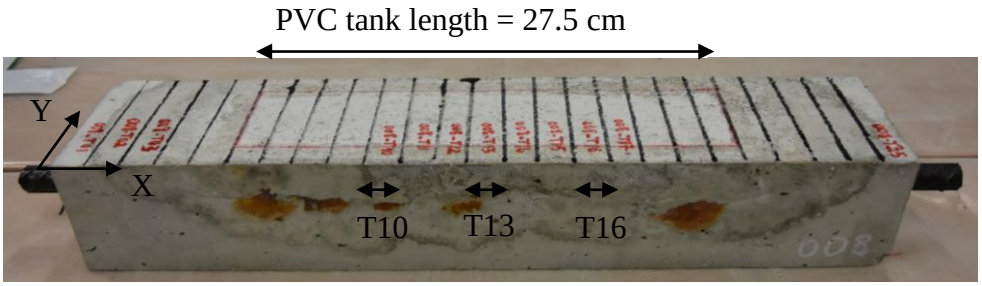

Figure 4. Specimen sawing design (25 slices named Tn° according to the axis. Corrosion test zone is between x=10 and x= 40 cm

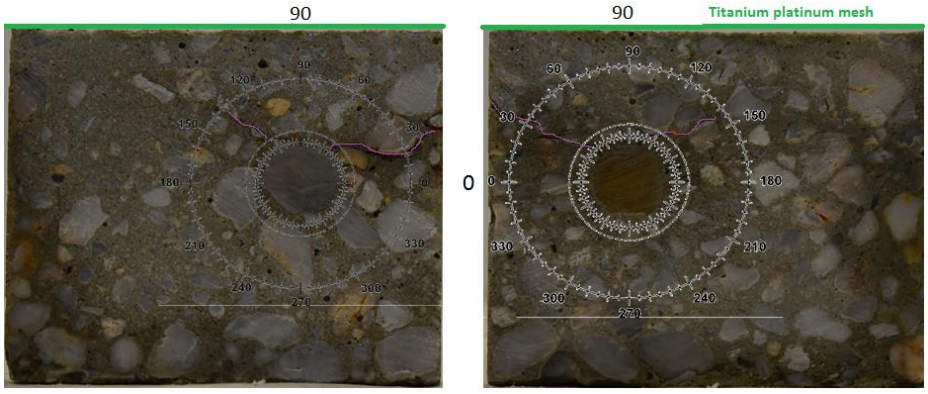

(a)

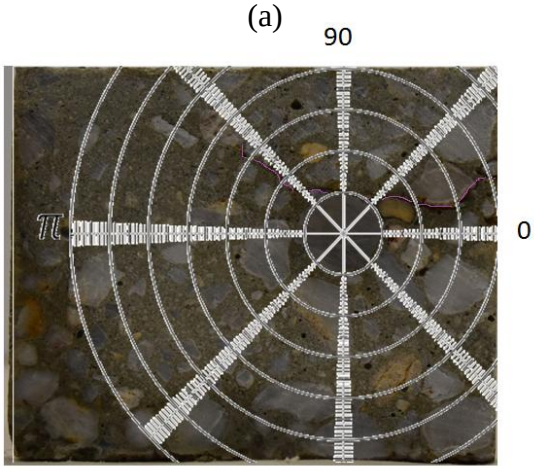

(b)

Figure 5. Determination of the crack angular position (a) and the crack length (b) after the accelerated corrosion test on the two sections of a slice

3 Experimental results

3.1 Voltage evolution during the accelerated corrosion test

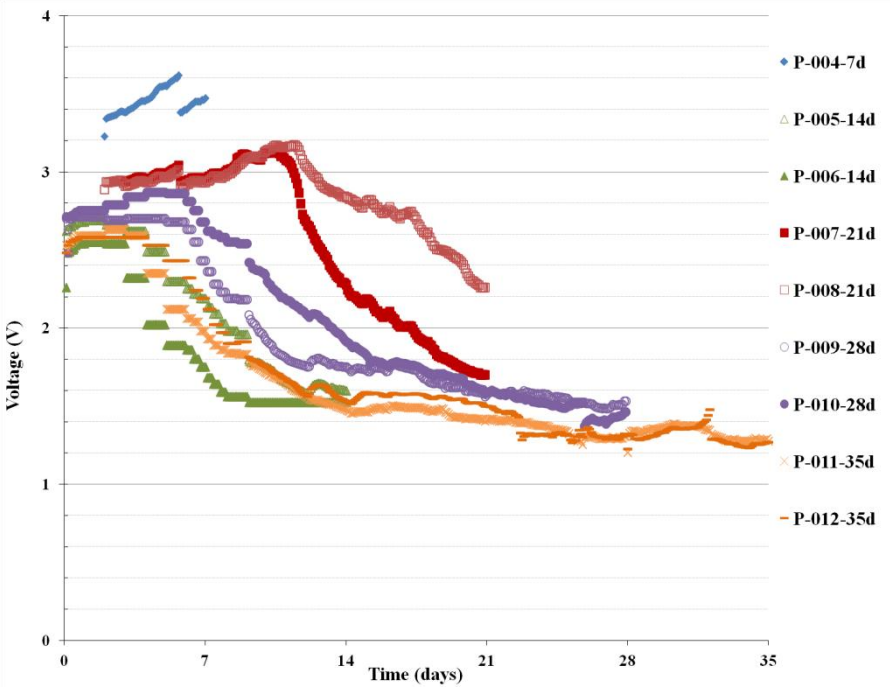

Figure 6. Voltage evolution during the accelerated corrosion test

[Figure 6] shows the voltage evolution for each RC specimen subjected to the accelerated corrosion test versus time. Before the test (time=0), the voltage reflects the electrical resistance of the specimens which are in a close range from 2.5 to 3 V except for P004-7d specimen (3.3V). During the test, three stages are observed. In the first stage, the voltage increase (about 1V) may be explained by the formation of resistive iron oxides (passive layer) [9], [10] around the rebar and also by the diffusion into the concrete and the filling up of the concrete pores by the oxides in the vicinity of the steel. In the second step, the drastic voltage decrease (50% loss) can arise from the concrete cracking and the steel / concrete debonding. The last stage with a constant voltage (1.4V) appears for longer durations, 28d and 35d and is likely representative of a constant impedance of the corrosion layer. These preliminary observations need to be discussed considering the migration of the ionic species under current and particularly the penetration of the chloride ions. Tests are under progress.

3.2 Corrosion rate and crack patterns

[Figure 7] shows the corrosion signs and the cracks observed for the top side and the front side of the two specimens after an accelerated corrosion test of 21 days.

Regarding the top sides, specimen P-007 shows some corrosion product stains and a visible crack roughly along the steel rebar whereas specimen P-008 is not damaged. Regarding the

front sides, the opposite behaviour is observed: specimen P-007 only exhibits a single spot of corrosion product while specimen P-008 shows significant corrosion products along the crack that follows the rebar. An assumption to explain this difference could be that the aggregate as well as the rebar's ribs are not homogeneously distributed and promote this heterogeneity.

Top side P-007-21d

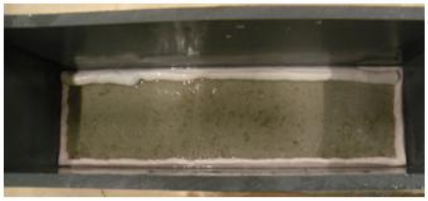

Top side P-008-21d

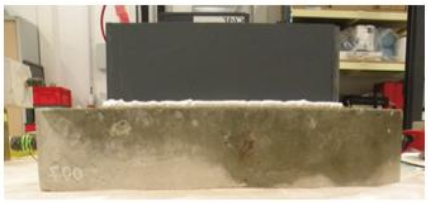

Front side P-007-21d

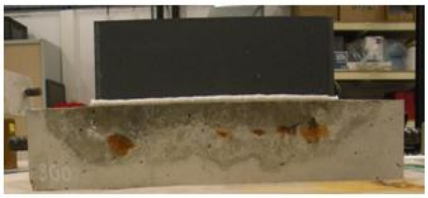

Front side P-008-21d

Figure 7. Qualitative results of the specimens after an accelerated corrosion of 21 days

[Figure 8] reveals that all corroded specimens for over 14 days have a J_{corr} equal to 10 µA/cm² approximately except the specimen P-004-7d corroded for 7 days. The proposed assumption is that at 7 days chloride ions have not reached the steel/concrete interface yet and consequently, the corrosion is still passive. To give an answer to this question, chloride measurement ingress with $AgNO_3$ will be achieved on each slice. Regarding the crack width, the behaviour of corroded specimens is different. As previously mentioned, all specimens are not cracked on the same side. As already suggested, this difference could be ascribed to the heterogeneity of the concrete (the random distribution of the aggregates into the cement paste). Besides, the crack on the top side is wider than the one on the front side. This observation might be attributed to the close localization of the counter electrode on the top side of the specimen (by comparison with the steel rebar) that permits chloride ions to quickly reach the rebar (modification of the physico-chemical conditions that locally enhances the corrosion process).

[Figure 9] shows the evaluation of the crack patterns (angular position (a), length (b) and width (c)) for each of the 10 cross-sections of the five slices of specimen P-008-21d. The cracks propagate from the steel/concrete interface to the concrete surface.

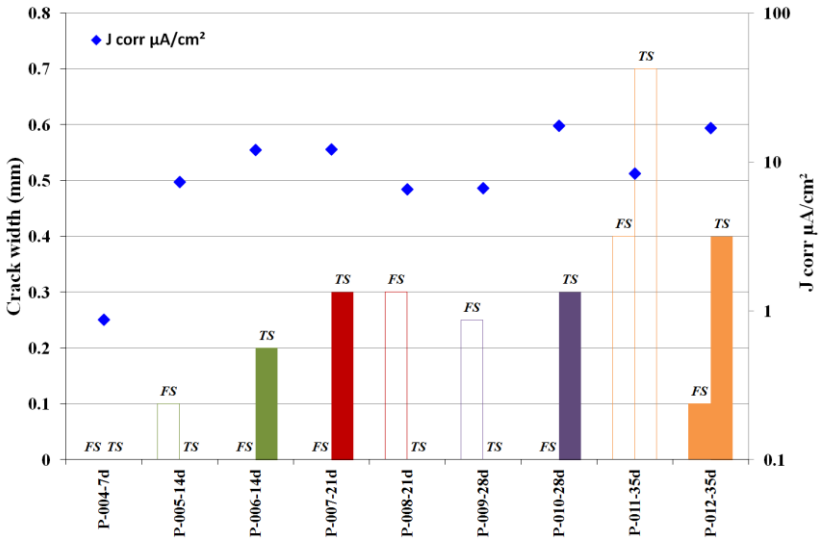

Figure 8. Crack width evolution and J_{corr} *(FS:front side ; TS:top side)*

As shown in [Figure 9-a], two groups of the position of the cracks near the steel surface are observed oriented close to 40° and 120° according to the graduated circle (see [Figure 5-a]). Two mains cracks seem to be displayed. Two sets of crack lengths could be identified, the first one is between 2 and 3cm and the second one is between 1 and 2cm in [Figure 9-b]. The lengths tend to fluctuate because of the distribution of the aggregates which influences the crack path. The graph in [Figure 9-c] corresponds to crack widths and shows the observed general trend. The crack widths are around 0.1 and 0.3mm.

The thickness of corrosion products is measured by Scanning Electron Microscopy and the perimeter represents the length of the shape of the rebar according to the corrosion volume.

The minimum thickness of corrosion products varies from 50 to 57µm and the maximum thickness varies from 257 to 314µm (see Table 1). The highest thickness is located in the upper part of the steel rebar. This ‘expected’ difference could result from the distance between the counter electrode and the steel surface area. The closer they get, the more the corrosion is forced. The crack width located on the top side is wider than the one located on the front side because the penetration path of the chloride ions to reach the steel surface area is the shortest.

Comparing the internal measurements ‘crack orientations’ and the widths measured on the sliced samples to the external observations (corrosion products spots on the front side of the samples), the surface observations do not reflect the internal corrosion state at the steel/concrete interface.

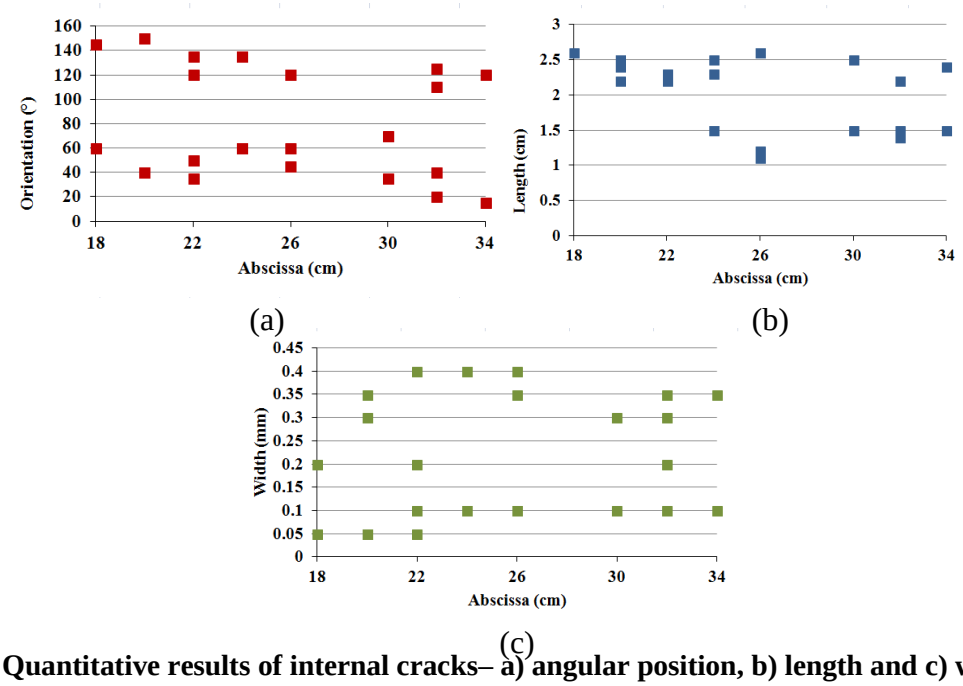

Figure 9. Quantitative results of internal cracks– a) angular position, b) length and c) width

Table 1 : Thickness of the corrosion products layers and corresponding visual distribution of evidences on the front side

Slices	Maximum thickness of the corrosion products layers (µm)	Minimum thickness of the corrosion products layers (µm)	Perimeter of the corrosion products layers Max/Min (µm)
P-008-21d-T10	257	57	2 617 / 5 233
P-008-21d-T13	314	63	5 233 / 5 233
P-008-21d-T16	257	50	5 233 / 10 467

4 Conclusions

In this work, cracks due to the corrosion of the steel reinforcement in concrete specimens have been investigated using an accelerated corrosion test. This work exposes the finalized methodology associated with the experimental program. The following preliminary results can be drawn:

- There are three stages in the corrosion process: during the first stage, the increase of polarization resistance may be explained by the development of resistive iron oxides (passivation layer). The second stage could highlight the loss of the resistance of the set due to respectively the concrete cracking and the decohesion between the steel and concrete surface area. Regarding the third stage, the observed effect may be attributed to the fact that the properties of corrosion layers remain unchanged. Then, the value of the voltage at the end of the test certainly reflects the resistance of both cracked

concrete cover and iron oxide layer. After 7 days, an active corrosion is not clearly observed and this could be explained by the fact that chloride ions have not reached the steel/concrete interface.

- The crack orientation, length and width are coherent for the same specimen corroded for 21 days. This result has to be confirmed after achieving the measurements for the other specimens.
- The corrosion-product spots on the surface of the samples do not reflect the internal corrosion state at the steel/concrete interface of the specimen.

Some of the experimental results such as the thickness and the display of the oxide layer will be used as input data for the numerical modelling. The other experimental results associated to the crack patterns will allow a comparison between the experience and the modelling. To improve the modelling of the corrosion product layer in the numerical simulation, an experimental test is in progress to characterize mechanical properties of these products.

5 References

[1] Cairns, J. and S. Millard, *Reinforcement corrosion and its effect on residual strength of concrete structures*, in *8 th International Conference Structural Faults+Repair-99*. 1999: London.

[2] weyers, R. and B. Prowell, *Corrosion inhibiting repair and rehabilitation treatment process for reinforced concrete structures.* Cement and Concrete Composites, 1996: p. 459.

[3] Mehta, P.K. and P.J.M. Monteiro, in *Concrete: structures, Properties and Materials.* 1997, Indian Concrete institute: India.

[4] Jamali, A., et al., *Modeling of corrosion-induced concrete cover cracking: A critical analysis.* Construction and Building Materials, 2013. **42**: p. 225-237.

[5] Dehoux, A., *Propriétés mécaniques des couches de produits de corrosion à l'interface acier / béton*. 2012, Université Pierre et Marie Curie.

[6] AFNOR(2001) , N.E.-. *Testing hardened concrete. Part 6: Tensile splitting strength of test specimens*. 2001.

[7] AFNOR (2003), NF EN 12390-3., *Testing hardened concrete. Part 3: Compressive strength of test specimens Andrade C., Alonso C. and Molina F. (1993), "Cover cracking as a function of bar corrosion: part I – experimental test", Materials and Structures.* **26**: p. 453-464.

[8] Sanz Merino, B., *Experimental and numerical study of cracking of concrete due to corrosion*. 2014, Universidad Politecnica de Madrid Escuela Tecnica Superior de Ingeniros de Caminos, Canales y Puertos. p. 254.

[9] Caré, S. and A. Raharinaivo, *Influence of impressed current on the initiation of damage in reinforced mortar due to corrosion of embedded steel.* Science Direct, 2007. **37**: p. 1598-1612.

[10] Poupard, O., *Corrosion by chlorides in reinforced concrete: Determination of chloride concentration threshold by impedance spectroscopy.* Cement and Concret Reasearch, 2004. **34**: p. 991-1000.